2014 5th IEEE RAS & EMBS International Conference on
Biomedical Robotics and Biomechatronics (BioRob)
August 12-15, 2014. São Paulo, Brazil

Bipedal Walking Gait with Variable Stiffness Knees

Wesley Roozing and Raffaella Carloni

Abstract— **The Segmented Spring-Loaded Inverted Pendulum model is analysed, and it is shown that it exhibits walking gait. We propose a control architecture that exploits control of the knee stiffness to provide robustness of the system with respect to changes in gait. This controller is extended for a realistic bipedal robot model that uses variable stiffness actuators to control the knee stiffness. The variable knee stiffness is then used to stabilise the system into a walking gait and to inject energy losses generated by friction and foot impacts.**

I. INTRODUCTION

The high performance of human walking, which combines robustness with energy efficiency, has long been the inspiration of efforts to design robots based on the principle of passive dynamic walking. In contrast, most existing systems are either energy efficient or robust. Robots based on the principle of passive dynamic walking show high energy efficiency, but are not robust against external disturbances [1]. Highly controlled systems – often based on the concept of Zero Moment Point – are robust at the exchange of energy efficiency [2].

Humans walking on flat terrain can be accurately modeled using inverted spring-mass systems. The Spring-Loaded Inverted Pendulum (SLIP) has been shown to exhibit autonomous stable limit cycle walking gait [3] strongly comparable to human walking in terms of hip trajectory, single- and double-support phases and ground contact forces [4].

In this work, we focus on the Segmented Spring-Loaded Inverted Pendulum (S-SLIP) model, which has segmented legs with torsional stiffness knees. This is more realistic when compared with existing robot designs, which use knees and leg retraction to avoid food scuffing. It has been shown that given proper initial conditions, the uncontrolled S-SLIP model exhibits autonomous stable limit cycle running gait [5]. However, the model also shows passive limit cycle walking gait, similar to the SLIP model.

We develop a control strategy that uses variable knee stiffness to stabilise the system with respect to changes of walking gaits, characterised by different limit cycles. The performance of this strategy is shown by a simulated S-SLIP system with controlled torsional knee stiffness that switches between two gaits with a large forward velocity difference.

Wesley Roozing is within the Department of Advanced Robotics, Istituto Italiano di Tecnologia, via Morego, 30, 16163 Genova. Email: wesley.roozing@iit.it (Research performed at the MIRA Institute, Faculty of Electrical Engineering, Mathematics, and Computer Science, University of Twente, The Netherlands). Raffaella Carloni is within the MIRA Institute, Faculty of Electrical Engineering, Mathematics, and Computer Science, University of Twente, The Netherlands. Email: r.carloni@utwente.nl

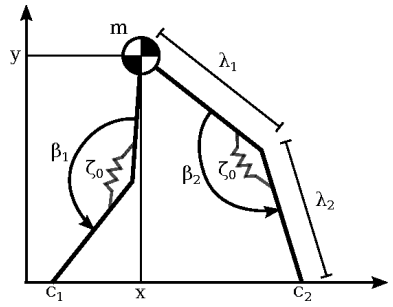

Fig. 1. The S-SLIP model consists of a hip point mass, with two massless segmented legs with links of length λ_1 and λ_2. In the knees with angles β_1 and β_2 there are torsional springs with stiffness ζ_0. The legs touch the ground at the foot contact points c_1 and c_2.

In the context of applying this control strategy to bipedal robots, a realistic model is designed that uses variable stiffness actuators (VSAs) to control the knees. The control is based on the developed strategy for the controlled S-SLIP model, extended with additional components to facilitate leg swing and leg retraction, which arise due to the additional dynamics of this model. A reference gait is obtained by using this model with constant knee stiffness. The variable knee stiffness is then used to stabilise the system into this gait and to inject the energy lost due to friction and foot impacts. It is shown that this results in a stable limit cycle walking gait.

The remainder of this paper is outlined as follows. Section II describes the S-SLIP model and its dynamics. The proposed control design for the S-SLIP model is described in Section III, with simulations in Section IV. The bipedal robot model is presented in Section V, its control in Section VI, and simulations in Section VII. Conclusions and recommendations for future work are presented in Section VIII.

II. SEGMENTED SPRING-LOADED INVERTED PENDULUM

In this section, the S-SLIP model is described. We describe the configuration manifold and conditions for state transition. The system dynamics are derived and we conclude with S-SLIP limit cycle gaits in a normalised description.

A. Configuration Manifold & State Transitions

The Segmented Spring-Loaded Inverted Pendulum (S-SLIP) model is shown in Fig. 1. It consists of a hip point mass m, connected to two massless segmented legs, each composed of two links with upper leg length λ_1 and lower leg length λ_2. Between the links there are torsional springs with stiffness ζ_0, and the knee angles are denoted by β_1 and β_2. The foot contact positions are denoted by c_1 and c_2.

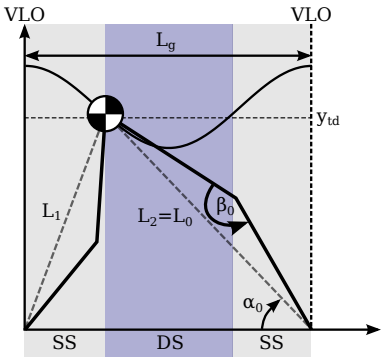

Fig. 2. A single step of the S-SLIP model, shown at touch-down. The leading leg is at its knee rest angle β_0. The virtual leg from hip to foot contact (dashed line) is at its rest length L_0 and at an angle α_0 with the ground plane. The step starts and ends at VLO and has length L_g. The virtual leg lengths are defined as L_1 and L_2. Touch-down and lift-off occur when the hip mass crosses the touch-down height y_{td}.

The configuration of the system is given by the position of the hip mass as $(x, y) =: \mathbf{q} \in \mathcal{Q}$, and its velocity by $\dot{\mathbf{q}} \in T_{\mathbf{q}}\mathcal{Q}$, the tangent space to $\mathcal{Q}$ at $\mathbf{q}$. The system state is then given as $\mathbf{x} := (\mathbf{q}, \mathbf{p})$, with the momentum $\mathbf{p} := (p_x, p_y) = M\dot{\mathbf{q}}$ and the mass matrix $M = \mathrm{diag}(m, m)$.

As in [3] and [6], a single step is defined as a trajectory $\mathbf{q}(t) \in \mathcal{Q}$ that starts with the system in Vertical Leg Orientation (VLO), where the hip mass is exactly above the supporting leg and $c_1 = x$. The step ends when the system again reaches VLO (see Fig. 2), and the role of the legs is then exchanged. We define the gait length $L_g := x(T)$, where T is the gait time period, i.e. $\mathbf{q}(t) = \mathbf{q}(t + T)$.

Every step consists of two distinct phases, i.e. single-support (SS) and double-support (DS) during which either one or two legs are in contact with the ground, respectively. The SS→DS transition occurs when the hip mass reaches the touch-down height y_{td}. The touch-down height corresponds to the angle-of-attack α_0, at which the virtual leading leg (from hip to foot contact, dashed lines in Fig. 2) is at an angle α_0 with the ground so that $y = y_{td} := L_0 \sin(\alpha_0)$. At this moment the leading leg is at its rest length L_0 and the knee is at its rest angle β_0:

$$L_0 = \sqrt{\lambda_1^2 + \lambda_2^2 - 2\lambda_1\lambda_2 \cos(\beta_0)} \tag{1}$$

At the moment of touch-down the leading foot contact position is calculated, as $c_2 = x + L_0 \cos(\alpha_0)$.

Conversely, the DS→SS transition occurs when the trailing virtual leg reaches its rest length. At this moment foot contact c_2 is relabeled as c_1 to correspond to the notation used during SS phase. The swing leg disappears, and reappears at the subsequent moment of touch-down, which is possible because the leg is massless. During SS we set the swing leg knee to its rest angle, i.e. $\beta_2 \equiv \beta_0$ and the leg exerts no force.

We can now define two subsets of $\mathcal{Q}$ which correspond to the single- and double-support phases respectively:

$$\begin{aligned} \mathcal{Q}_{SS} &= \{\mathbf{q} \in \mathcal{Q} \,|\, y > y_{td}\,,\; y < L_0\} \\ \mathcal{Q}_{DS} &= \{\mathbf{q} \in \mathcal{Q} \,|\, y < y_{td}\,,\; y > 0\} \end{aligned} \tag{2}$$

where the conditions $y < L_0$ and $y > 0$ assure to avoid the remaining cases, i.e. lift-off and fall respectively. Note that for a walking gait $\mathbf{q} \in \mathcal{Q}_{SS} \cup \mathcal{Q}_{DS}$. [1]

During contact, the length L_i of each leg is given by

$$L_i = \sqrt{(x - c_i)^2 + y^2}\,, \quad i \in \{1, 2\} \tag{3}$$

with corresponding knee angle β_i

$$\beta_i = \cos^{-1}\left(\frac{\lambda_1^2 + \lambda_2^2 - L_i^2}{2\lambda_1\lambda_2}\right),\; i \in \{1, 2\} \tag{4}$$

B. System Dynamics

To derive the dynamic equations for the system, we use the Hamiltonian approach. The kinetic energy function is defined as $K = \frac{1}{2}\mathbf{p}^T M^{-1}\mathbf{p}$ with $M := \mathrm{diag}(m, m)$ and the potential energy function as

$$V = mgy + \frac{1}{2}\zeta_0 (\beta_0 - \beta_1)^2 + \frac{1}{2}\zeta_0 (\beta_0 - \beta_2)^2$$

where g is the gravitational acceleration. The dynamic equations are then defined by the Hamiltonian energy function $H = K + V$ as

$$\frac{\mathrm{d}}{\mathrm{d}t}\begin{bmatrix}\mathbf{q}\\ \mathbf{p}\end{bmatrix} = \begin{bmatrix}0 & I\\ -I & 0\end{bmatrix}\begin{bmatrix}\frac{\partial H}{\partial \mathbf{q}}\\ \frac{\partial H}{\partial \mathbf{p}}\end{bmatrix} \tag{5}$$

where I is the identity matrix. Note that a solution $\mathbf{q}(t)$ of (5) is of class C^2, due to the non-differentiability of the leg forces at the moment of transition between the single- and double-support phases.

C. S-SLIP Limit Cycle Gaits

A limit cycle gait is a periodic walking gait, which returns to the same state periodically. From this point on, we refer to limit cycle walking gaits of the S-SLIP model as *natural gaits*. In the description of natural gaits, we use the state at VLO as initial conditions, i.e. $\mathbf{x}_0 = (\mathbf{q}, \mathbf{p})_0 = (x, y, p_x, p_y)_0$, and, during walking in natural gait, the system returns to this state at every VLO. Since we can take at every VLO $x \equiv 0$, a natural gait Σ can then be fully described as

$$\Sigma = (\alpha_0, \zeta_0, L_0, m, \beta_0, y_0, p_{x,0}, p_{y,0}) \tag{6}$$

in which we consider m and L_0 fixed parameters for a given system. Note that it is not possible to use the total system energy H to uniquely describe a natural gait, because energy can be stored in either potential (leg compression, hip height) or kinetic energy.

As natural gaits exist for ranges of parameters, there often exists a range of natural gaits that achieve a desired forward velocity. In Fig. 3, this corresponds to multiple combinations of $(\alpha_0, \zeta_0, \beta_0)$ that result in the same average forward velocity $\dot{x}_{avg}$. Conversely, a single set $(\alpha_0, \zeta_0, \beta_0)$ can often achieve a range of average forward velocities (vertical bar in Fig. 3). Given these parameters, a natural gait can be found by finding an initial state $\mathbf{x}_0$ to which the system returns at every VLO.

[1] Lift-off is also possible while $\mathbf{q} \in \mathcal{Q}_{SS} \cup \mathcal{Q}_{DS}$. We take care of this in simulation by checking $L_1 \leq L_0 \vee L_2 \leq L_0$, i.e. at least one leg is in contact with the ground.

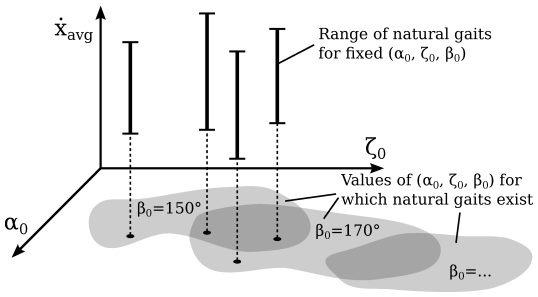

Fig. 3. Average forward velocities $\dot{\mathbf{x}}_{avg}$ of natural gaits for different values of $(\alpha_0, \zeta_0, \beta_0)$. Note that for given $(\alpha_0, \zeta_0, \beta_0)$, the average forward velocity is proportional to the system energy H.

D. Normalised Notation of S-SLIP Limit Cycle Gaits

The torsional knee stiffness ζ_0 and energy H can be normalised in dimensionless form as

$$\tilde{\zeta} = \frac{\zeta_0}{mgL_0} \qquad \tilde{H} = \frac{H}{mgL_0} \tag{7}$$

If we normalise $\mathbf{x}$ as $\tilde{\mathbf{x}} := (\tilde{\mathbf{q}}, \tilde{\mathbf{p}}) = (\tilde{x}, \tilde{y}, \tilde{p}_x, \tilde{p}_y)$ with

$$\tilde{x} = \frac{x}{L_0} \quad \tilde{y} = \frac{y}{L_0} \quad \tilde{p}_x = \frac{p_x}{m\sqrt{L_0 g}} \quad \tilde{p}_y = \frac{p_y}{m\sqrt{L_0 g}} \tag{8}$$

which are all dimensionless quantities, and use (7), we obtain a fully normalised unique description $\tilde{\Sigma}$ of a natural gait:

$$\tilde{\Sigma} = \left(\alpha_0, \tilde{\zeta}, \beta_0, \tilde{y}_0, \tilde{p}_{x,0}, \tilde{p}_{y,0}\right) \tag{9}$$

The gait trajectory can then be found by solving (5) for $\tilde{\Sigma}$. Using this description, equal gaits on different S-SLIP systems now result in the same normalised state trajectory $\tilde{\mathbf{x}}(t) = (\tilde{\mathbf{q}}(t), \tilde{\mathbf{p}}(t))$. Similarly to $\tilde{p}_x, \tilde{p}_y$, the velocities are normalised as

$$\dot{\tilde{x}} = \frac{\dot{x}}{\sqrt{L_0 g}} \qquad \dot{\tilde{y}} = \frac{\dot{y}}{\sqrt{L_0 g}} \tag{10}$$

Note that the normalisation $\dot{\tilde{x}}$ is the Froude number *Fr* [8], [9], used to compare the relative walking speeds of systems with different leg lengths.

III. S-SLIP CONTROL DESIGN

The control design of the controlled S-SLIP model is inspired by [6], in which the stiffness of the legs of the SLIP model is actively controlled and the rejection of external disturbances to the system is significantly increased.

Analogously, for the S-SLIP model, the torsional knee stiffness can be controlled. The knee stiffnesses in Fig. 1 are replaced by $\zeta_i = \zeta_0 + u_i, i \in \{1, 2\}$. The control inputs u_i are restricted to subsets $U_i = \{u_i \in \mathbb{R} | 0 < \zeta_0 + u_i < \infty\}$, such that the result is a meaningful stiffness value.

We intend to control the system towards a reference gait $\tilde{\Sigma}$ with normalised state trajectory $\tilde{\mathbf{x}}^o(t)$ such that $u_i \to 0, i \in \{1, 2\}$ as $t \to \infty$. To change gait we can then construct $\tilde{\mathbf{x}}^o(t)$ such that it converges from some reference gait $\tilde{\Sigma}_i$ to another $\tilde{\Sigma}_j$. However, during single-support phase the system has only one control input and $\tilde{\mathbf{x}}^o(t)$ cannot be tracked exactly, which may lead to instability as the system lags behind the reference. As $\tilde{x}$ was identified to be a periodic variable and required to be monotonically increasing in time, the references are reparametrised on $\tilde{x}$. The references $\tilde{y}^*(\tilde{x}), \dot{\tilde{x}}^*(\tilde{x})$ are then sufficiently described as

$$\tilde{y}^*(\tilde{x}) = \tilde{y}^o(\tilde{x}) \qquad \dot{\tilde{x}}^*(\tilde{x}) = \dot{\tilde{x}}^o(\tilde{x}) \tag{11}$$

However, as a general analytic expression for the spring-loaded pendulum does not exist [10], a Fourier series expansion approximation of the numerical solution is used. We extend (5) to obtain

$$\frac{\mathrm{d}}{\mathrm{d}t}\begin{bmatrix}\mathbf{q}\\ \mathbf{p}\end{bmatrix} = \begin{bmatrix}0 & I\\ -I & 0\end{bmatrix}\begin{bmatrix}\frac{\partial H}{\partial \mathbf{q}}\\ \frac{\partial H}{\partial \mathbf{p}}\end{bmatrix} + \begin{bmatrix}0\\ B\end{bmatrix}\mathbf{u} \tag{12}$$

with $\mathbf{u} = [u_1, u_2]$ the controlled part of the knee stiffness. The input matrix B is given by

$$B = \begin{bmatrix}\frac{\partial \phi_1}{\partial x} & \frac{\partial \phi_2}{\partial x}\\ \frac{\partial \phi_1}{\partial y} & \frac{\partial \phi_2}{\partial y}\end{bmatrix} \tag{13}$$

with

$$\phi_i = \frac{1}{2}\left(\beta_0 - \beta_i\right)^2, \quad i \in \{1, 2\} \tag{14}$$

calculated from (3)–(4). To formulate the control strategy, we rewrite (12) as

$$\dot{\mathbf{x}} = f(\mathbf{x}) + \sum_i g_i(\mathbf{x}) u_i \tag{15}$$

and then define error functions h_1 and h_2 as

$$\begin{aligned} h_1 &= y - y^* \\ h_2 &= \dot{x} - \dot{x}^* \end{aligned} \tag{16}$$

Due to only one control input being available during single-support phase, the system is not always fully controllable and we choose to:

1) Control the hip height error h_1 during SS around VLO
2) Control the velocity error h_2 during SS just after touch-down and just before lift-off.
3) Control both h_1 and h_2 during DS

We choose to control the velocity error just after lift-off and just before touch-down to allow generation of the required push-off for energy injection.

The control solution is then given as follows.

- For $\mathbf{q} \in \mathcal{Q}_{SS}$ and $|x - c_1| \leq \epsilon$:

$$\begin{aligned} u_1 &= \frac{1}{\mathcal{L}_{g_1}\mathcal{L}_f h_1}\left(-\mathcal{L}_f^2 h_1 - \kappa_d \mathcal{L}_f h_1 - \kappa_p h_1\right) \\ u_2 &\equiv 0 \end{aligned} \tag{17}$$

- For $\mathbf{q} \in \mathcal{Q}_{SS}$ and $|x - c_1| > \epsilon$:

$$\begin{aligned} u_1 &= \frac{1}{\mathcal{L}_{g_1} h_2}\left(-\mathcal{L}_f h_2 - \kappa_v h_2\right) \\ u_2 &\equiv 0 \end{aligned} \tag{18}$$

- For $\mathbf{q} \in \mathcal{Q}_{DS}$:

$$\begin{bmatrix}u_1\\ u_2\end{bmatrix} = A^{-1}\begin{bmatrix}-\mathcal{L}_f^2 h_1 - \kappa_d \mathcal{L}_f h_1 - \kappa_p h_1\\ -\mathcal{L}_f h_2 - \kappa_v h_2\end{bmatrix} \tag{19}$$

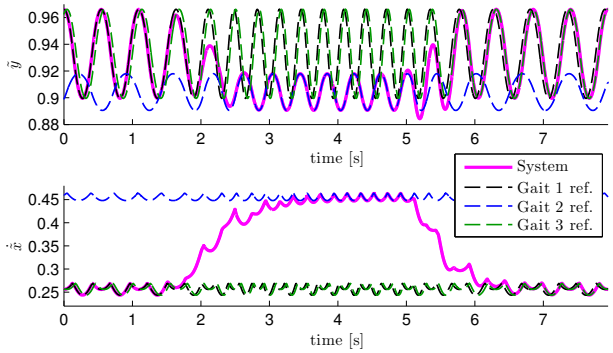

Fig. 4. Hip height and forward velocity over time. The system converges to the new gait in approximately 5 steps.

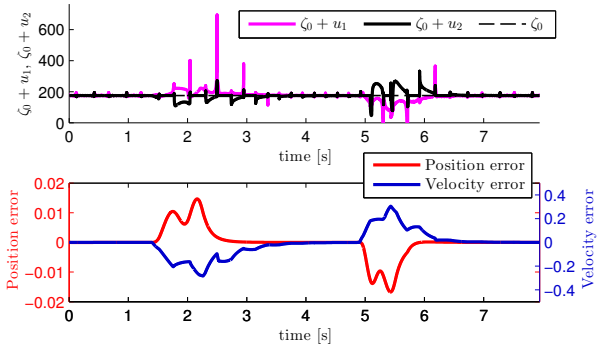

Fig. 5. Control input and error functions. The knee stiffness converges to the nominal value after rejection of the transition disturbances.

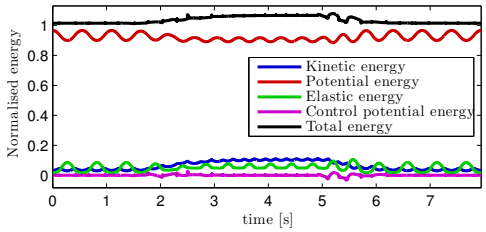

Fig. 6. Energy balance. The total energy increases on transition to the second gait, mostly reflected in kinetic energy increase resulting from the increased forward velocity.

with

$$A = \begin{bmatrix} \mathcal{L}_{g_1}\mathcal{L}_f h_1 & \mathcal{L}_{g_2}\mathcal{L}_f h_1 \\ \mathcal{L}_{g_1}\mathcal{L}_f h_2 & \mathcal{L}_{g_2}\mathcal{L}_f h_2 \end{bmatrix} \tag{20}$$

where $\mathcal{L}_f^2 h_i$, $\mathcal{L}_f h_i$, $\mathcal{L}_{g_i} h_i$ and $\mathcal{L}_{g_i}\mathcal{L}_f h_i$ denote the (repeated) Lie-derivatives of h_i along the vector fields defined in (15), $\kappa_d, \kappa_p, \kappa_v$ are tunable control parameters and $\epsilon \in [0, \frac{1}{2}L_g]$ is the distance around VLO during which h_1 is controlled.

The control inputs (17), (18), (19) ensure that the error h_1 converges asymptotically to zero and that the error h_2 is at least bounded [6].

Remark: The control inputs u_1, u_2 in (17)–(19) are continuous. However, their continuity is not guaranteed at the moment of transition.

IV. CONTROLLED S-SLIP SIMULATION RESULTS

To show the robustness of the method with respect to forward velocity differences, a slow gait with an average velocity of Fr = 0.259 (0.811 m s^{-1}) and $(\alpha_0, \tilde{\zeta}) = (70, 0.224)$, and a fast gait with an average velocity of Fr = 0.457 (1.429 m s^{-1}) and $(\alpha_0, \tilde{\zeta}) = (65, 0.224)$ are chosen. Furthermore, $m = 80$ kg, $\lambda_1 = \lambda_2 = 0.50$ m and $\beta_0 = 170$ deg (s.t. $L_0 \approx 0.996$ m), parameters which correspond roughly to humans. For the S-SLIP controller we set $\{\epsilon, \kappa_p, \kappa_d, \kappa_v\} = \{0.1, 50, 25, 50\}$, found using multiple simulation runs. From $\tilde{\zeta} = 0.224$ follows $\zeta_0 \approx 175$ N m rad^{-1}. Simulations were performed in Mathworks MATLAB R2012b, using the ode45 solver with absolute and relative tolerances of 1e-11.

The system starts in the slow gait (gait 1), is commanded to change to fast gait (gait 2) at 1.0 m, and then to switch back to the slow gait (gait 3 = gait 1) at 5.5 m. The controller references are produced using the switching method in [11].

Fig. 4 shows the hip height and forward velocity over time, which converge to the new gait in approximately 5 steps. Fig. 5 shows the corresponding control input and error functions. After transition the knee stiffnesses converge to the nominal value. Fig. 6 shows the energy balance. Most of the total energy increase on transition is put into kinetic energy, to accommodate the faster gait.

In the next section the control strategy proposed for the S-SLIP model is extended, to accommodate the additional dynamics of a realistic bipedal robot walker.

V. BIPEDAL ROBOT MODEL

The bipedal robot model is based on the mechanical design of an existing bipedal walker [7] and is modeled in the 20-sim 3D Mechanics Toolbox (Controllab Products B.V., The Netherlands) as depicted in Fig. 7. It is a four-link model with segments of length λ_1 and λ_2 similar to the S-SLIP model. However, conversely to the S-SLIP model, the swing leg does not disappear during swing, and its dynamics should be included in the model.

The hip mass is replaced by two separate upper-leg masses $m_{h,l}, m_{h,r}$ – there is a small mass difference on the physical robot due to a guide rail on the left side – with rotational inertias $J_{h,l}, J_{h,r}$, and two lower-leg masses m_l with rotational inertias J_l are added (Fig. 8). The hip joint position is denoted by (x, y), and we denote the angles of attack of the virtual legs by α_l, α_r. Similarly, the knee joint angles are denoted by β_l, β_r respectively. The angle-of-attack of the virtual stance leg (during SS) or leading virtual leg (during DS) is always denoted as α. The hip angle is denoted by θ.

There are three control inputs to the system: hip torque τ_h, left knee torque τ_l and right knee torque τ_r. The hip torque is generated by a realistic motor and gearbox model and the knee torques are generated by variable stiffness actuator (VSA) models. VSAs belong to a class of actuators which are able to change their apparent output stiffness independently of their output equilibrium position by proper control of their internal degrees of freedom. In this work a model of the vsaUT-II is used [12].

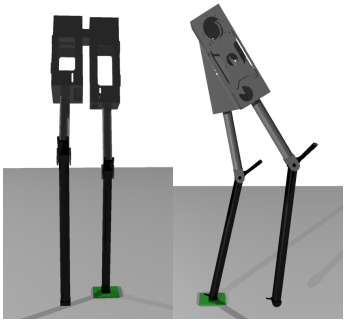

Fig. 7. The bipedal robot model is based on the mechanical design of a bipedal walker in our lab, with realistic body dynamics, friction and ground contact forces.

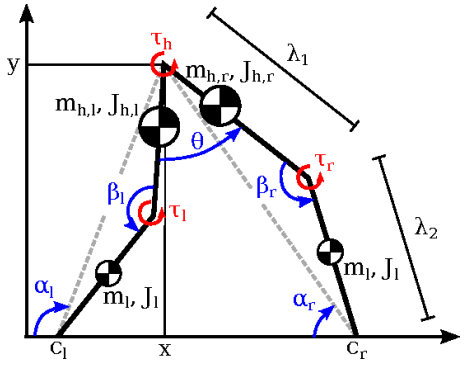

Fig. 8. Bipedal robot model. The model is similar to the S-SLIP model, with the hip mass replaced by two upper-leg masses and the addition of two lower-leg masses.

The foot contact positions are denoted by c_l, c_r and the ground contact forces are modeled using the Hunt-Crossley contact model. The robot is constrained to the sagittal plane using constraint forces.

VI. BIPEDAL ROBOT CONTROL DESIGN

A. Controller Structure

The proposed controller structure of the bipedal robot is shown in Fig. 9. The controller determines the robot configuration and phase from angle measurements and foot contact sensors. For the SS stance leg and DS, the controller uses the knee stiffness control strategy developed for the S-SLIP model as presented in Sec. III. During stiffness control

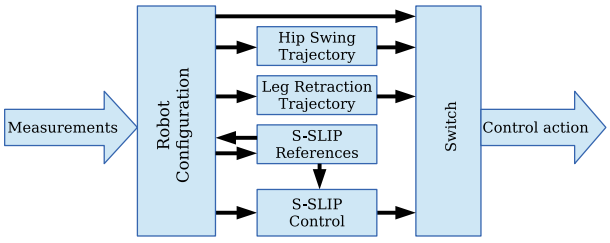

Fig. 9. Proposed controller structure. The controller switches between constant-stiffness trajectory control and stiffness control for each of the knees depending on the phase. During leg swing, the hip and leg retraction trajectories are generated using minimum-jerk trajectories.

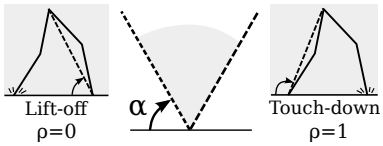

Fig. 10. During single-support phase the hip swing and leg retraction are parametrised using the variable ρ, with $\rho = 0$ at lift-off and $\rho = 1$ at the expected moment of touch-down.

the equilibrium position of both knees is set to β_0, i.e. the knee rest angle, to obtain the desired stiffness behaviour. The swing leg is controlled using constant-stiffness trajectory control of the knee for leg retraction. The hip swing and leg retraction trajectories are generated using minimum-jerk trajectories, parametrised by a variable ρ (Sec. VI-B).

B. Step Parametrisation

For control of the hip swing and leg retraction, each step is parametrised from lift-off to subsequent touch-down using the variable ρ (Fig. 10). We define $\rho \equiv 0$ at lift-off, and $\rho \equiv 1$ at the expected moment of touch-down. We define ρ as a function of the angle-of-attack of the current stance leg α, set to either $\alpha = \alpha_l$ (left stance) or $\alpha = \alpha_r$ (right stance):

$$\rho = \begin{cases} 0 & \alpha \leq \alpha_{lo} \\ (\alpha - \alpha_{lo})/(\alpha_{td} - \alpha_{lo}) & \text{otherwise} \\ 1 & \alpha \geq \alpha_{td} \end{cases} \tag{21}$$

such that given $\alpha_{td} > \alpha_{lo}$, $\rho \in [0, 1]$. We calculate $\alpha_{lo} = \alpha$ at the moment of lift-off to ensure continuous behaviour. The value of α at the expected moment of touch-down is obtained from the reference S-SLIP model as α_{td}. To ensure continuity, the value of ρ is also calculated during flight phase using the leg last in contact.

C. Hip Swing

The desired hip trajectory $\theta^*(\rho)$ is generated using a minimum-jerk trajectory, with boundary conditions

$$\begin{pmatrix} \theta^*(0) \\ \theta^*(1) \end{pmatrix} = \begin{pmatrix} \theta_{lo} \\ \theta_{td} \end{pmatrix} \tag{22}$$

where θ_{lo} is the hip angle calculated at the moment of swing leg lift-off and θ_{td} is the hip angle expected to result in the desired angle-of-attack of the swing leg, calculated as $\theta_{td} = \alpha_0 - \alpha_{td}$.

D. Leg Retraction

The leg retraction trajectory is generated similarly to the hip swing. However, the leg is kept retracted for a period during the swing to avoid foot scuffing.

The desired knee angle β of the swing leg is given as

$$\beta^*(\rho) = \begin{cases} r_1(\rho) & 0 < \rho < 0.3 \\ \beta_{ret} & 0.3 \leq \rho \leq 0.6 \\ r_2(\rho) & 0.6 < \rho \leq 0.85 \\ \beta_0 & 0.85 < \rho < 1 \end{cases} \tag{23}$$

where β_{ret} is the retracted knee angle and $r_1(\rho), r_2(\rho)$ are minimum-jerk trajectories which control β^* from β_0 to β_{ret}

TABLE I

BIPEDAL ROBOT MODEL PARAMETERS

$m_{h,l}$	7.511	[kg]	m_l	0.779	[kg]
m_{h_r}	6.848	[kg]	ζ_0	196.6	[N m rad^{-1}]
λ_1	0.515	[m]	λ_2	0.495	[m]
β_0	160	[deg]	α_0	70	[deg]
β_{ret}	137.5	[deg]	α_{td}	98.3	[deg]

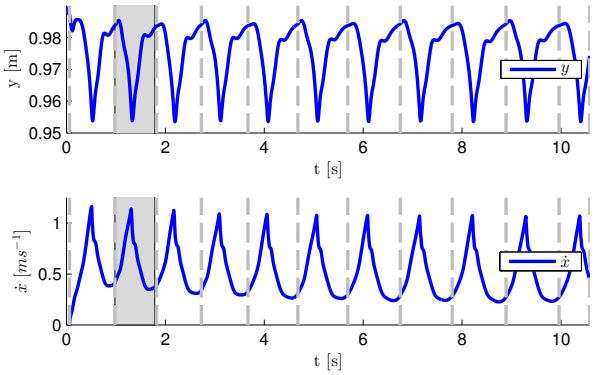

Fig. 11. Walking behaviour with constant knee stiffness. Vertical dashed lines indicate VLO. The shaded area indicates the step that was used for reference gait approximation. The average gait velocity is decreasing as time progresses, as there is no energy injected through variable knee stiffness.

and from β_{ret} to β_0, respectively. The domains in (23) were chosen such that the leg is quickly retracted to avoid foot scuffing, and has reached its extended position before touch-down.

VII. BIPEDAL ROBOT MODEL RESULTS

The bipedal robot was simulated using the Vode Adams integrator with absolute and relative tolerances of 1e-8. The system parameters are as in Table I.

A. Gait Reference

To obtain the gait reference for the bipedal robot model, the system was given a constant knee stiffness ζ_0 (i.e. S-SLIP knee stiffness control turned off) and a small push forward to start walking. This way only leg swing and leg retraction are controlled using ρ, i.e. there is no dependency on the parametrised reference and the behaviour is mainly governed by leg swing dynamics. The resulting walking behaviour is shown in Fig. 11. Vertical dashed lines indicate VLO and the system starts in left stance VLO.

Walking starts with an average forward velocity of ≈ 0.7 m s^{-1}, however the average gait velocity is decreasing as time progresses, and, eventually, the system comes to a standstill. Thus only the hip swing is not injecting sufficient energy to compensate for losses and we don't converge to limit cycle behaviour. We approximate the gait reference using the hip trajectory of the second step by Fourier series (Fig. 11).

B. Walking Results

We now enable the S-SLIP knee stiffness controller. We again set $\{\epsilon, \kappa_p, \kappa_d, \kappa_v\} = \{0.1, 50, 25, 50\}$. Fig. 12 shows the walking behaviour of the system after walking for some

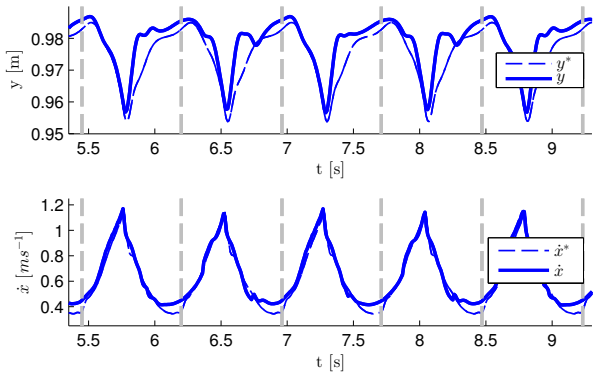

Fig. 12. Stable walking gait with controlled knee stiffness. Vertical dashed lines indicate VLO. The knee stiffness control successfully injects the lost energy every step.

time. The system converges to a stable walking gait. Knee stiffness control successfully injects the lost energy every step, keeping the mean energy over every step constant, resulting in constant average velocity. Some asymmetry remains between left and right stance, due to the mass asymmetry. This is reflected in the inputs and errors (Fig. 13), as the reference was created out of a step during right stance there is a larger error and control inputs during left stance. The hip height error is below 1.5 cm and the velocity error is below 0.1 m s^{-1}. The control inputs are limited to $u_l, u_r \in [-\zeta_0, 1000]$ N m rad^{-1}. The average forward velocity during the shown interval is 0.65 m s^{-1}, corresponding to a Froude number *Fr* of ≈ 0.21. In comparison, "Veronica" [8] achieves speeds ranging from an *Fr* of 0.07 to 0.16, and "Meta" [9] achieves an *Fr* of 0.1 to 0.28.

The SS velocity control law (18) generates high control inputs, especially during touch-down and left-foot push-off. This results from the orientation of the leg in these cases and low compression of the leg. The actuator power corresponding to the control inputs are shown in Fig. 14. Hip actuator power is below 60 W. VSA Stiffness control power is generally below 20 W. The power required to change the knee equilibrium position has peaks up to 150 W due to the short leg retraction and extension time and low retraction angle. These values are within the limits of the motors of the physical robot, although we did not account for efficiency overhead of the mechanical implementation of the VSAs [12].

VIII. CONCLUSIONS AND FUTURE WORK

We have analysed the dynamics of the S-SLIP system and developed a control strategy based on variable knee stiffness that is robust enough to handle changes in the gait, i.e., able to control the system from one limit cycle walking gait to another. It was shown that the controller can switch gait by injecting or removing energy from the system appropriately, after which control inputs converge to zero.

Towards a control strategy for bipedal robots to change gait, a bipedal robot model with realistic dynamics was designed. The S-SLIP control strategy was extended to

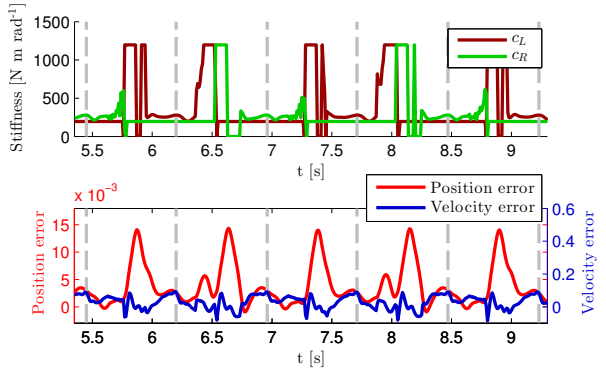

Fig. 13. Control inputs and errors. As the reference was created out of a step during right stance, there is a larger error and control inputs during left stance. The hip height disturbance arising from foot push-off during velocity control is quickly rejected during mid-stance position control.

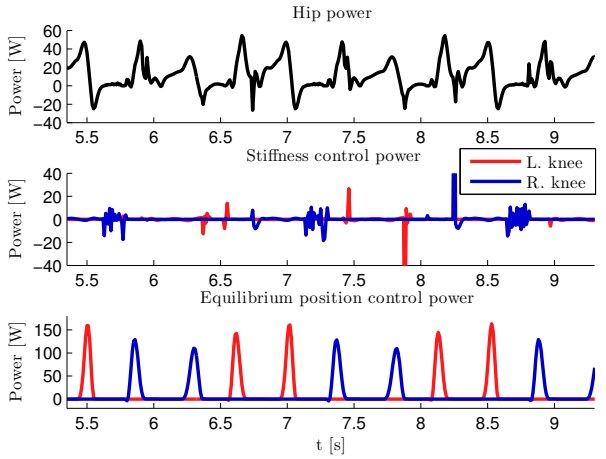

Fig. 14. Hip and VSA power. Hip power is below 60 W. VSA stiffness control power is generally below 20 W. The power required to change the knee equilibrium position has peaks up to 150 W due to the short leg retraction and extension time and low retraction angle.

facilitate hip swing and leg retraction. To obtain the desired stiffness behaviour together with adjustable knee equilibrium position for leg retraction, variable stiffness actuators have been used. The gait reference was obtained from the constant-stiffness walking behaviour of the system. Simulated experiments show the controller successfully injects energy lost due to friction and foot impacts and the system converges to limit cycle walking gait.

In the presented results a constant high knee stiffness was used to obtain the reference gait, however gaits with lower knee stiffness could make better use of the compliant leg behaviour, storing mechanical energy and thus making the gait more energy efficient. Furthermore, our results showed that the moment of touch-down is important, mainly due to the explicit dependency on a gait reference parametrised in forward position. In the case of disturbances this may lead to the system running out of phase with the reference. Parametrisation of the reference w.r.t. the orientation of the current stance leg or touch-down events should be considered in the future.

Future work will focus on further improving the control strategy and implementation on the experimental setup.

REFERENCES

[1] T. McGeer, "Passive dynamic walking," *The International Journal of Robotics Research*, vol. 9, no. 2, pp. 62–82, 1990.

[2] S. Collins and A. Ruina, "A bipedal walking robot with efficient and human-like gait," *IEEE International Conference on Robotics and Automation*, 2005.

[3] J. Rummel, Y. Blum, and A. Seyfarth, "Robust and efficient walking with spring-like legs," *Bioinspiration and Biomimetics*, vol. 5, no. 4, p. 16, 2010.

[4] H. Geyer, A. Seyfarth, and R. Blickhan, "Compliant leg behaviour explains basic dynamics of walking and running," *The Royal Society B, Biological Sciences*, vol. 273, no. 1603, pp. 2861–7, 2006.

[5] J. Rummel and A. Seyfarth, "Stable Running with Segmented Legs," *The International Journal of Robotics Research*, vol. 27, no. 8, pp. 919–934, 2008.

[6] L. C. Visser, S. Stramigioli, and R. Carloni, "Robust Bipedal Walking with Variable Leg Stiffness," *IEEE RAS/EMBS International Conference on Biomedical Robotics and Biomechatronics*, 2012.

[7] J. G. Ketelaar, L. C. Visser, S. Stramigioli, and R. Carloni, "Controller design for a bipedal walking robot using variable stiffness actuators," *IEEE International Conference on Robotics and Automation*, 2013.

[8] Y. Huang, B. Vanderborght, R. Van Ham, Q. Wang, M. Van Damme, G. Xie, and D. Lefeber, "Step Length and Velocity Control of a Dynamic Bipedal Walking Robot With Adaptable Compliant Joints," *IEEE/ASME Transactions on Mechatronics*, vol. 18, no. 2, pp. 598–611, 2013.

[9] D. G. E. Hobbelen and M. Wisse, "Controlling the Walking Speed in Limit Cycle Walking," *The International Journal of Robotics Research*, vol. 27, no. 9, pp. 989–1005, 2008.

[10] S. V. Kuznetsov, "The motion of the elastic pendulum," *Regular and Chaotic Dynamics*, vol. 4, no. 3, pp. 3–12, 1999.

[11] W. Roozing, L. C. Visser, and R. Carloni, "Variable Bipedal Walking Gait with Variable Leg Stiffness," *IEEE RAS/EMBS International Conference on Biomedical Robotics and Biomechatronics*, 2014.

[12] S. S. Groothuis, G. Rusticelli, A. Zucchelli, S. Stramigioli, and R. Carloni, "The vsaUT-II: a Novel Rotational Variable Stiffness Actuator," *IEEE International Conference on Robotics and Automation*, 2012.